

# Position control of DC motor using fractional order controller

ANDRZEJ RUSZEWSKI, ANDRZEJ SOBOLEWSKI

*Faculty of Electrical Engineering  
Białystok University of Technology  
e-mail: {andrusz/soboland}@pb.edu.pl*

(Received: 12.08.2012, revised: 29.01.2013)

**Abstract:** The paper presents the problem of position control of DC motor with rated voltage 24 V loaded by flywheel. The fractional order PD controller implemented in National Instruments NI ELVIS II programmed in LabView is used for controlling. The simple method for determining stability regions in the controller parameters space is given. Knowledge of these regions permits tuning of the controller and ensures required the phase margin of the system.

**Key words:** position, DC motor, controller, fractional order

## 1. Introduction

In recent years considerable attention has been paid to fractional calculus and its application in many areas in science and engineering (see, e.g. [4, 7, 9, 12]).

In control system fractional order controllers are used to improve the performance of the feedback control loop. The fractional PID controllers, namely  $PI^\lambda D^\mu$  controllers, including an integrator of  $\lambda$  order and a differentiator of  $\mu$  order were proposed in [15, 16]. The problem of tuning the  $PI^\lambda D^\mu$  controllers have been presented in the literature (see, e.g. [5, 6, 8, 10, 11, 18, 23]). The asymptotic stability is the basic requirement of a closed-loop system. Some methods for determining the asymptotic stability regions in the fractional controller parameter space were proposed in [8, 17]. Gain and phase margins are measures of relative stability for a feedback system. For example, in paper [18] a simple method of determining the stability region (satisfying the conditions of gain and phase margins) in the parameter space of a fractional order inertial plant with time delay and a fractional order PID controller was given.

In order to implement (digital realization) of the fractional order controller the approximate time rational transfer function should be determined. Some methods of obtaining the discrete transfer function approximating the continuous fractional order transfer function have been proposed in the literature [12-14, 20-22]. Generally, the digital transfer function is based on the canonical form of the infinite impulse response filter (IIR filter). Such an algorithm can be

directly implemented into any processor based devices as for instance programmable logic controller (PLC) [13, 14].

In this work the problem of position control of DC motor loaded by flywheel is presented. The considered DC-motor is a component of the system QUANSER DC Motor Position Control (DCMPC). The fractional order PD controller implemented in the device National Instruments NI ELVIS II programmed in the graphical environment LabView is used. The parametric synthesis of the controller is carried out using the proposed method for determining the stability regions in the controller parameter space for the specified phase margin of the system. The controlled object is modeled as the transfer function of the inertia with integration. The comparative studies of this control system are presented.

## 2. Controlled system

The DC Motor Position Control system shown in Figure 1 consists of a direct-current motor with an inertia wheel on the motor shaft with rotor inertia  $20 \text{ gcm}^2$ . The nominal output power of the motor is 12.98 W and the maximal rotational speed reaches 7500 rpm with speed constant 685 rpm/V. The angular position of the motor shaft is measured by an optical encoder with a resolution of approximately  $0.0879^\circ$ . Due to the resolution of the encoder and the use of the 24 bit counter, the range of values that can be read by the encoder is approximately  $\pm 4096 \cdot 2\pi$ . The motor is driven using a pulse-width modulated (PWM) power amplifier. The maximum output voltage of the amplifier is 24 V.

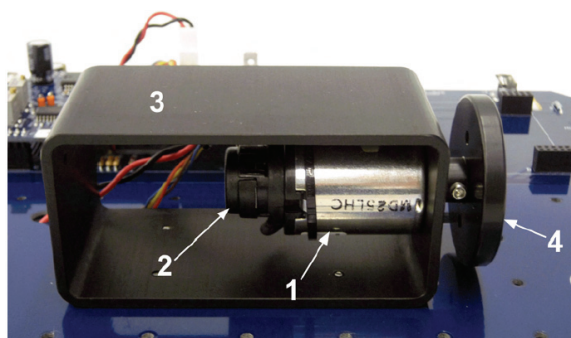


Fig. 1. DCMPC system and controlled object: 1) DC motor, 2) encoder, 3) motor metal chamber, 4) Inertial load

The step-test method is used for accurate plant modeling for control system analysis and design. This model is compared with the measured response by running the simulation and actual system in parallel. The model parameters are tuned for a better fit. The identification of the motor model parameters is performed using 2 V step input in an open-loop. Figure 2 shows the comparison of the model and the motor response characteristics which are carried out for sampling time 5 ms.

The resulting model is a transfer function from voltage to motor shaft position

$$G(s) = \frac{K}{s(\tau s + 1)}, \quad K > 0, \quad \tau > 0, \quad (1)$$

where  $K$  is the steady-state gain, and  $\tau$  is the time constant.

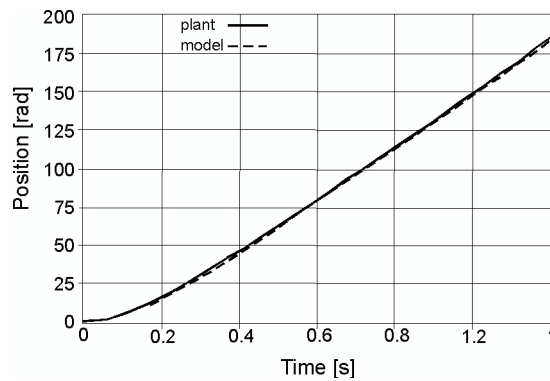


Fig. 2. Step responses of plant and its model with step input 2 V

The experimentally obtained step response of the system is approximated to the step response of the model (1) with the parameters  $K = 35$  [rad/sV] and  $\tau = 0.15$  [s].

### 3. Fractional order PID controller

The fractional order  $PI^\lambda D^\mu$  controller [15, 16] was proposed as a generalization of the PID controller [2] with integrator of real order  $\lambda$  and differentiator of real order  $\mu$ . The transfer function of such a type controller in the Laplace domain takes the form

$$C(s) = k_p + k_i s^{-\lambda} + k_d s^\mu, \quad \lambda > 0, \quad \mu > 0, \quad (2)$$

where  $k_p$ ,  $k_i$  and  $k_d$  denote the proportional, integral and differential gains of the controller respectively.  $k_p$ ,  $k_i$  and  $k_d$  parameters usually take non-negative values.

Taking  $\lambda = 1$  and  $\mu = 1$  we obtain a classical PID controller. If  $k_d = 0$  or  $k_i = 0$  we obtain a  $PI^\lambda$  controller or  $PD^\mu$  controller, respectively. All these types of controllers are particular cases of the  $PI^\lambda D^\mu$  controller. In this paper we use the  $PD^\mu$  controller, whose transfer function has the form

$$C(s) = k_p + k_d s^\mu. \quad (3)$$

The block diagram of the considered feedback control system is shown in Figure 3, where  $G(s)$  has form (1) and  $C(s)$  has form (3).

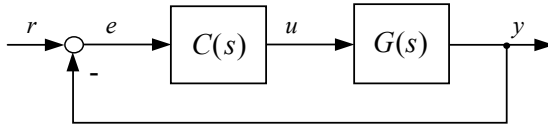


Fig. 3. Feedback control system structure

### 3.1. Parametric synthesis of the controller

The asymptotic stability is the basic requirement of a closed-loop system. Gain and phase margins are measures of relative stability for a feedback system, therefore the synthesis of control systems is very often based on them. In typical control systems the phase margin is from  $30^\circ$  to  $60^\circ$  whereas the gain margin is from 5 dB to 10 dB.

In this paper we tuning the controller for the specified phase margin, because a phase margin is closely related to a transient response, i.e. overshoot. For this purpose we use the phase margin tester  $\exp(-j\phi)$ , where  $\phi$  is a phase margin. This tester does not exist in the real control system, it is only used for the controller tuning.

Taking into account the phase margin tester  $\exp(-j\phi)$  in the main path of control, plant (1) and controller (3) we obtain the characteristic polynomial of the closed-loop system

$$w(s) = e^{-j\phi} K (k_p + k_d s^\mu) + s(s\tau + 1). \quad (4)$$

Using the classical  $D$ -partition method the stability region in the parameter plane  $(k_d, k_p)$  may be determined and the parameters can be specified. The stability boundaries are curves on which each point corresponds to polynomial (4) having zeros on the imaginary axis. It may be the real zero boundary or the complex zero boundary. It is easy to see that polynomial (4) has zero  $s = 0$  if  $k_p = 0$  (the real zero boundary). The complex zero boundary corresponds to the pure imaginary zeros of (4). We obtain this boundary by solving the equation

$$w(j\omega) = e^{-j\phi} K (k_p + k_d (j\omega)^\mu) + j\omega(j\omega\tau + 1) = 0, \quad (5)$$

which we get by substituting  $s = j\omega$  in polynomial (4) and equating to 0. The complex Equation (5) can be rewritten as a set of real equations in the form

$$\operatorname{Re}[w(j\omega)] = 0, \quad \operatorname{Im}[w(j\omega)] = 0. \quad (6)$$

where  $\operatorname{Re}[w(j\omega)]$  and  $\operatorname{Im}[w(j\omega)]$  denote the real and the imaginary parts of (5), respectively. Finally, by solving the Equations (6) we obtain

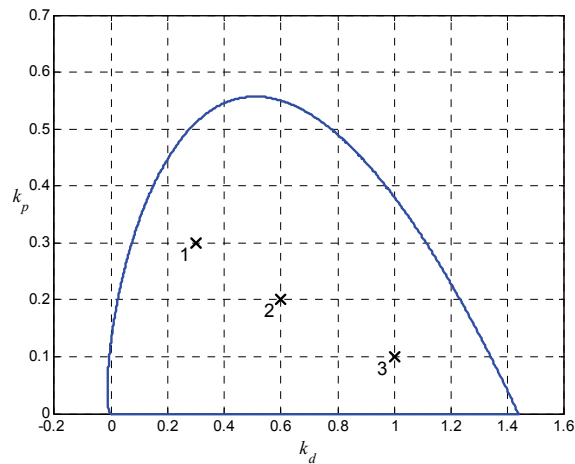
$$k_d = \omega^{1-\mu} \frac{\omega\tau \sin \phi - \cos \phi}{K \sin\left(\frac{\pi}{2}\mu\right)}, \quad (7)$$

$$k_p = \omega \frac{\omega\tau \sin\left(\frac{\pi}{2}\mu - \phi\right) + \cos\left(\frac{\pi}{2}\mu - \phi\right)}{K \sin\left(\frac{\pi}{2}\mu\right)}. \quad (8)$$

Equations (7) and (8) determine the complex zero boundary as a function of  $\omega$ . The real zero boundary and the complex zero boundary for  $\omega \geq 0$  decompose plane  $(k_d, k_p)$  into some regions. The stability region is chosen by testing an arbitrary point from each region and checking the stability of polynomial (4). In this paper only the stability region in the parameter plane of polynomial (4) is presented. When the stability regions are known, the tuning of the fractional controller can be carried out.

On computing complex and real zero boundaries by the proposed method, we obtain the stability regions in the controller parameter plane  $(k_d, k_p)$ . The stability regions for  $\phi = 60^\circ$ ,  $\mu = 0.6$  are shown in Figure 3. The complex boundary of stability regions is calculated for transfer function (1) with  $K = 35$  and  $\tau = 0.15$ . The stability region lies between line  $k_p = 0$  (the real zero boundary) and the curve assigned to specified phase margin  $\phi$  (the complex zero boundary). On choosing any point from the stability region we obtain the controller parameter values provided the phase margin of this system is greater than that specified for drawing the complex boundary. Any point from the stability region provides a phase margin of this system greater than  $60^\circ$ . The value of  $\mu = 0.6$  is chosen as an example.

Fig. 4. Stability regions for  $\phi = 60^\circ$ ,  $\mu = 0.6$



The controller parameters and stability margins of the control system for all points marked in Figure 4 are listed in Table 1. It is shown that the stability margin values are greater than that specified for drawing the complex boundary of the stability region. Table 1 confirms that points from the stability regions satisfy the phase margin requirements.

Table 1. Controller parameters and phase margins

Point	Controller parameters	Phase margin [°]
1	$k_d = 0.3, k_p = 0.3, \mu = 0.6$	64.5
2	$k_d = 0.6, k_p = 0.2, \mu = 0.6$	63.2
3	$k_d = 1.0, k_p = 0.1, \mu = 0.6$	61.3

### 3.2. Digital realization of the fractional order controller

Transfer functions (2) and (3) of the controller are the irrational functions in the variable  $s$ . Therefore, accurate physical realization of the differentiation and integration of a fractional order is not possible. In order to implement the fractional order controller the approximate time rational transfer function should be determined. The approximate time rational transfer function may be in the form of a discrete transfer function with integral orders. Such a transfer function can be directly implemented into any processor based devices. Some methods of obtaining the discrete transfer function approximating the continuous fractional order transfer function have been proposed in the literature [12-14, 20-22].

In the paper [19] the realization of fractional order controller implemented in National Instruments sbRIO-9631 controller programmed in LabView was presented. In order to digitally realize the fractional order controller transfer function, operator-based continuous fraction expansion (CFE) scheme was applied. In this paper the same scheme is used, however the realization of fractional order PD $^\mu$  controller is implemented in National Instruments NI Elvis II device.

Transfer function (2) corresponds in the discrete domain to the discrete transfer function has the form

$$C(z^{-1}) = k_p + k_d (\varpi(z^{-1}))^\mu, \quad (9)$$

where the approximate transfer function of the differentiator of real order  $\mu$  has the form [13]

$$\begin{aligned} (\varpi(z^{-1}))^\mu &\approx \left(\frac{1+a}{T}\right)^\mu CFE \left\{ \left( \frac{1-z^{-1}}{1+az^{-1}} \right)^\mu \right\}_{p,q} = \\ &= \left(\frac{1+a}{T}\right)^\mu \frac{P(z^{-1})}{Q(z^{-1})} = \left(\frac{1+a}{T}\right)^\mu \frac{p_0 + p_1 z^{-1} + p_2 z^{-2} + \dots + p_m z^{-p}}{q_0 + q_1 z^{-1} + q_2 z^{-2} + \dots + q_m z^{-q}}. \end{aligned} \quad (10)$$

CFE{.} is the continued fraction expansion,  $P$  and  $Q$  are polynomials of degree  $p$  and  $q$ , respectively,  $a$  is ratio term and  $T$  is sampling time. Depending on the value of  $a = \{0, 1/7, 1\}$  we obtain Euler rule, Al-Alaoui rule and Tustin rule, respectively. Coefficients of  $P$  and  $Q$  polynomials depend to the order of the approximate model and we can calculate them from the following forms for  $p = q = 1$

$$p_0 = q_0 = \frac{2}{a + \mu + \mu a - 1}, \quad p_1 = \frac{a - \mu - \mu a - 1}{a + \mu + \mu a - 1}, \quad q_1 = 1, \quad (11)$$

whereas for  $p = q = 2$

$$\begin{aligned}
 p_0 = q_0 &= \frac{12}{a^2 \mu^2 + 3a^2 \mu + 2a\mu^2 + 2a^2 + \mu^2 - 8a - 3\mu + 2}, \\
 p_1 &= \frac{12a - 6\mu - 6a\mu - 12}{a^2 \mu^2 + 3a^2 \mu + 2a\mu^2 + 2a^2 + \mu^2 - 8a - 3\mu + 2}, \\
 p_2 &= \frac{a^2 \mu^2 - 3a^2 \mu + 2a\mu^2 + 2a^2 + \mu^2 - 8a + 3\mu + 2}{a^2 \mu^2 + 3a^2 \mu + 2a\mu^2 + 2a^2 + \mu^2 - 8a - 3\mu + 2}, \\
 q_1 &= \frac{12a + 6\mu + 6a\mu - 12}{a^2 \mu^2 + 3a^2 \mu + 2a\mu^2 + 2a^2 + \mu^2 - 8a - 3\mu + 2}, \\
 q_2 &= 1.
 \end{aligned} \tag{12}$$

The practical fractional controller realization is implemented in NI Elvis II device using the NI LabView graphical programming language. The program window for entering the values of controller parameters and approximation parameters is shown in Figure 5.

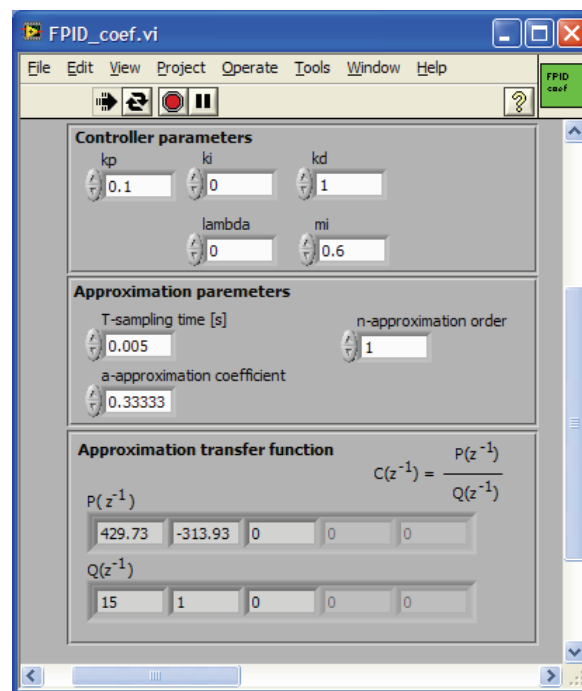


Fig. 5. Program window for setting up fractional control coefficients

One of the application feature is a set of controller parameters like  $k_p$ ,  $k_i$ ,  $k_d$ ,  $\lambda$ ,  $\mu$  and approximation parameters  $T$ ,  $a$ . All those data are used to determine coefficients of appro-

ximating discrete transfer function. For example, if the controller parameters are  $k_d = 1$ ,  $k_p = 0.1$ ,  $\mu = 0.6$  (point 3 in Tab. 1) and approximating coefficients are  $T = 0.005$ ,  $a = 0.333$ ,  $n = 1$  than the discrete transfer function approximating the continuous fractional order transfer function (3) has the form

$$C(z^{-1}) = \frac{429.73 - 313.93z^{-1}}{15 + z^{-1}}, \quad (13)$$

whereas for  $n = 2$ ,  $T = 0.005$  s,  $a = 0.333$  and the same values of controller parameters (point 3 in Table 1) the discrete transfer function (9) has the form

$$C(z^{-1}) = \frac{-244.78 + 260.42z^{-1} - 36.4z^{-2}}{-8.54 + 2.28z^{-1} + z^{-2}}. \quad (14)$$

The comparison of Bode characteristics for the continuous transfer function of controller (3) with  $k_d = 1$ ,  $k_p = 0.1$ ,  $\mu = 0.6$  and the discrete transfer functions (13) and (14) is shown in Figure 6.

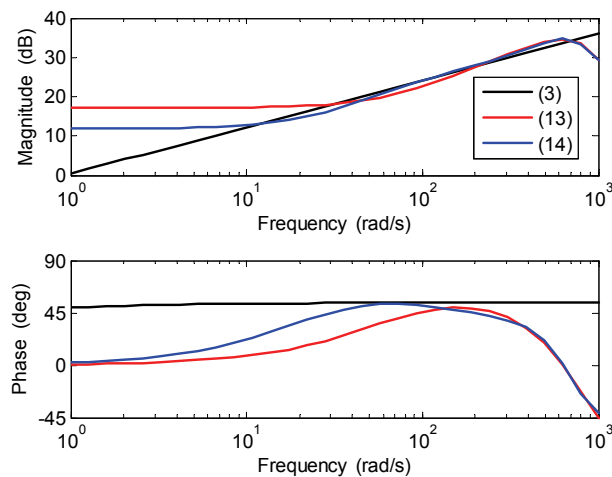


Fig. 6. Comparison of Bode plots of transfer functions (13), (14) and (3) with  $k_d = 1$ ,  $k_p = 0.1$ ,  $\mu = 0.6$ .

## 4. Experiments

The experiments made it possible to observe how the position control loop operates as a result of the set point changing from  $-2\pi$  to  $+2\pi$  radians. All experiments were carried out for sampling time  $T = 0.005$  s. The controller parameter values are chosen according to Table 1 which presents phase margin specifications (points marked in Fig. 4). Step responses of the system controlled by a practical implemented controller with  $n = 1$  and  $n = 2$  are shown in Figures 7 and 8, respectively. From these figures we can see that the order of approximation affects the character of step responses. When  $n = 1$  all responses are characterized by over-



shoot whereas all step responses obtained for  $n = 2$  are aperiodic. The system response for the control parameters corresponding the point 1 of Table 1 has the largest overshoot (Fig. 7).

Fig. 7. Step responses of the closed-loop system with the  $PD^\mu$  controller (approximation order  $n = 1$ )

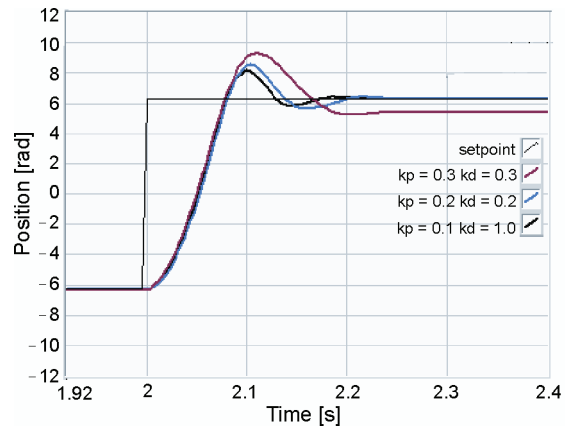


Fig. 8. Step responses of the closed-loop system with the  $PD^\mu$  controller (approximation order  $n = 2$ )

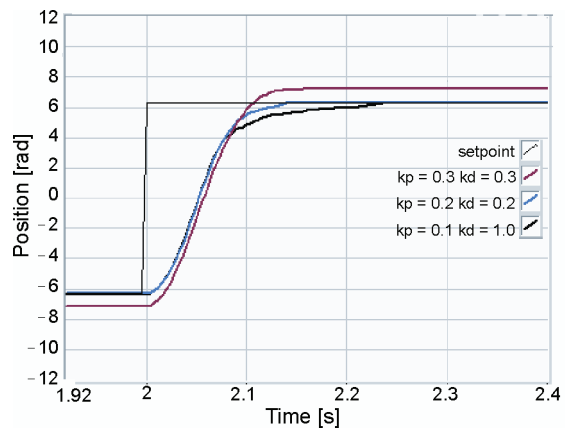
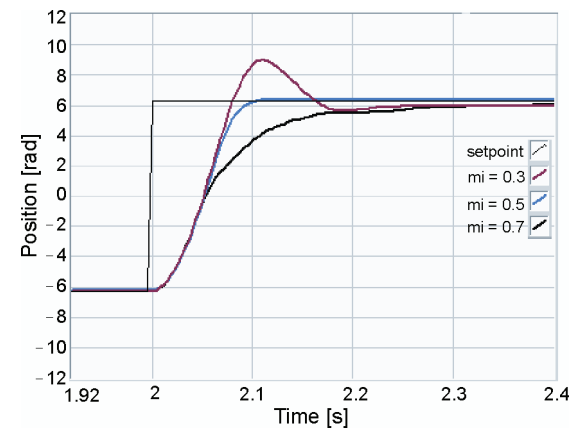
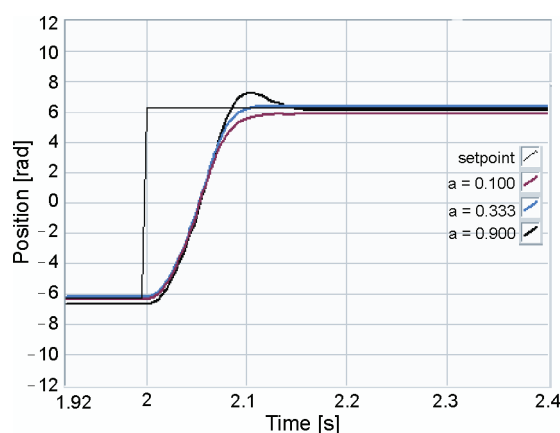


Fig. 9. Step responses of the closed-loop system with the  $PD^\mu$  controller related to  $\mu$  ( $n = 2$ )



In laboratory test bench is also examined the impact of value coefficient  $\mu$  on step responses. The controller parameters  $k_d$  and  $k_p$  are taken in accordance with point 3 of Table 1 and the value of  $\mu$  is varied. Exemplary time responses obtained for  $\mu = 0.3, 0.5, 0.7$  are shown in Figure 9. We can see the trend of changes in position characteristics versus values of coefficient  $\mu$ . The step response with the shortest settling time, the zero of steady state error and the lack of overshoot is obtained for  $\mu = 0.5$ . The figure shows that for smaller values of  $\mu$  (e.g.  $\mu = 0.3$ ) step responses are characterized by the overshoot.

Fig. 10. Step responses of the closed-loop system with the  $PD^\mu$  controller related to  $a$  ( $\mu = 0.5, n = 2$ )



Another examination refers to the influence of the approximation coefficient  $a$  on step responses. The controller parameters  $k_d$  and  $k_p$  are taken according to point 3 of Table 1 with the value of  $\mu = 0.5$ . Figure 10 shows the comparison of characteristics obtained for three values of the parameter  $a$ , i.e. 0.1, 0.333 and 0.9. We can see that a coefficient  $a$  has the significant effect on the overshoot and steady state error. The increasing value of  $a$  results in larger oscillations, whereas the decreasing causes a larger steady state error.

From Figures 9 and 10 we can see that the values of coefficient  $a$  and order  $\mu$  have a significant effect on the overshoot and steady state error.

## 5. Conclusion

In this paper the position control of DC motor shaft loaded by flywheel is given. The fractional order PD controller implemented into National Instruments NI ELVIS II device programmed in LabVIEW is used. The parametric synthesis of the fractional order PD controller was performed using the proposed method for determining the stability regions in the parameter space of the controller. Knowledge of these regions permits tuning of the controller and ensures required the phase margin of the system.

The results of experimental research confirm that the proposed implementation technique simplifies the process of determining digital realization of the continuous fractional order con-

troller. Thanks to graphical interface user is able to introduce fractional order controller gains and automatically determine the discrete transfer function approximating the continuous fractional order transfer function.

### Acknowledgments

The work was supported by the National Centre of Science in Poland under grant No. N N514 638940.

### References

- [1] Al-Alaoui M.A., *Filling the gap between the bilinear and the backward difference Transforms: an interactive design approach*. Int. J. Elect. Eng. Edu. 34(4): 331-337 (1997).
- [2] Astrom K.J., Hagglund T., *PID Controllers: Theory, Design, and Tuning*. 2nd ed. Research Triangle Park, NC: Instrument Society of America (1995).
- [3] Biswas A., Das, S, Abraham A., Dasgupta S., *Design of fractional-order  $PI^{\lambda}D^{\mu}$  controllers with an improved differential evolution*. Engineering Applications of Artificial Intelligence 22(2): 343-350 (2009).
- [4] Busłowicz M., *Selected problems of continuous-time linear systems of non-integer order*. Measurement Automation and Robotics 2: 93-114 (2010) (in Polish).
- [5] Caponetto R., Dongola G., Fortuna L., Gallo A., *New results on the synthesis of FO-PID controllers*. Communications in Nonlinear Science and Numerical Simulation 15(4): 997-1007 (2010).
- [6] Castillo J., Feliu V., Rivas R., Sanchez L., *Design of a class of fractional controllers from frequency specifications with guaranteed time domain behavior*, Computers and Mathematics with Applications 59(5): 1656-1666 (2010).
- [7] Das S., *Functional fractional calculus for system identification and controls*. Springer, Berlin (2008).
- [8] Hamamci S.E., *An algorithm for stabilization of fractional-order time delay systems using fractional-order PID controllers*, IEEE Trans. on Automatic Control 52: 1964-1969 (2007).
- [9] Kaczorek T., *Selected Problems of Fractional Systems Theory*. Springer, Berlin (2011).
- [10] Luo Y., Chen Y.Q., *Fractional order [proportional derivative] controller for a class of fractional order systems*. Automatica 45(10): 2446-2450 (2009).
- [11] Monje C.A., Vinagre B.M., Feliu V., Chen Y., *Tuning and auto-tuning of fractional order controllers for industry applications*. Control Engineering Practice 16: 798-812 (2008).
- [12] Ostalczyk P., *Epitome of the Fractional Calculus, Theory and its Applications in Automatics*. Publishing Department of Technical University of Łódź (2008) (in Polish).
- [13] Petras I., *Fractional-order feedback control of a DC motor*. Journal of Electrical Engineering 60(3): 117-128 (2009).
- [14] Petras I., *Realization of fractional-order controller based on PLC and its utilization to temperature control*. Transfer inovacii 14: 34-38 (2009).
- [15] Podlubny I., *Fractional differential equations*. Academic Press, San Diego (1999).
- [16] Podlubny I., *Fractional-order systems and  $PI^{\lambda}D^{\mu}$  controllers*. IEEE Trans. on Automatic Control 44: 208-214 (1999).
- [17] Ruszewski A., *Stability regions of closed loop system with time delay inertial plant of fractional order and fractional order PI controller*. Bull. Pol. Ac.: Sci. Tech. 56(4): 329-332 (2008).
- [18] Ruszewski A., *Stabilization of fractional-order inertial plants with time delay using fractional PID controllers*. Measurement Automation and Robotics 2: 406-414 (2009) (in Polish).
- [19] Ruszewski A., Sobolewski A., *Comparative studies of control systems with fractional controllers*. Przegląd Elektrotechniczny 88(4b): 204-208 (2012).
- [20] Tenreiro M., Galhano A.M., Oliveira A.M., Tar J.K., *Approximating fractional derivatives through the generalized mean*. Communications in Nonlinear Science and Numerical Simulation 14(11): 3723-3730 (2009).

- 
- [21] Vinagre B.M., Podlubny I., Hernandez A., Feliu V., *Some approximations of fractional order operators used in control theory and applications*. Fractional Calculus and Applied Analysis 3(3): 231-248 (2000).
- [22] Vinagre B.M., Chen Y.Q., Petras I., *Two direct Tustin discretization methods for fractional – order differentiator/integrator*. Journal of the Franklin Institute: Engineering and Applied Mathematics 340: 349-362 (2003).
- [23] Zhao C., Xue D., Chen Y.Q., *A fractional order PID tuning algorithm for a class of fractional order plants*. [In:] Proc. of the IEEE International Conference on Mechatronics & Automation, pp. 216-221, Niagara Falls, Canada (2005).